On-site full-scale tests of a timber queen-post truss

Jorge M. Branco[a], Humberto Varum[b], Filipe T. Matos[c]

[a] Assistant Professor, ISISE, Univ. of Minho, Dept. of Civil Engineering, Campus de Azurém, 4810-058 Guimarães, Portugal.
Tel. +351 253 510 200; Fax: +351 253 510 217
E-mail: jbranco@civil.uminho.pt; ***Corresponding author***

[b] Full Professor, CONSTRUCT-LESE, Faculty of Engineering, Univ. of Porto, Dept. of Civil Engineering
E-mail: hvarum@fe.up.pt

C PhD student, ISISE, Univ. of Minho, Dept. of Civil Engineering
E-mail: filipetmatos@gmail.com

ABSTRACT: On-site tests were performed on an existing traditional timber truss. The main goal of the tests was to evaluate the overall behavior of the timber truss under symmetric and non-symmetric vertical loading. Moreover, the influence of the location of the point loads application was assessed, with and without eccentricity relatively to the joints. The loading tests were preceded by a visual and non-destructive inspection aimed at collecting geometric data and assessing the level of decay of each member. The field tests results of a queen-post truss are presented and analyzed. A numerical model was developed to reproduce and analyse the test results.

1 INTRODUCTION

The lack of practical, yet realistic, numerical models for the simulation of the behavior of joints in traditional timber structures normally leads to the replacement of old roof structures, instead of their retrofitting, to satisfy safety and serviceability requirements present in recent Codes and Recommendations. Moreover, the misunderstanding of the global behavior of traditional timber roof structures can result in unacceptable stress distribution in the members, as a result of inappropriate joint strengthening (in terms of stiffness and/or strength). To overcome this need, laboratory tests on scaled or full-scale specimens of members, connections and trusses, can be done. However, the behavior in real conditions, in terms of materials and member connections, can be evaluated only via on-site testing.

Field tests on traditional timber trusses are not common. Researchers (Parisi and Piazza 2002; Del Senno 2003; Piazza et al., 2004; Branco et al. 2008; Branco et al. 2010; Barbari et al. 2014; Branco et al. 2017) have preferred to transport the full-scale specimens to a laboratory. Parisi and Piazza (2002) tested a full-scale roof truss (king-post truss

superimposed above queen-post truss) of Silver fir (*Abies alba* Mill.), of mid-19th century, to validate and calibrate a numerical model developed for the analysis of timber structures subjected to seismic forces. Branco et al. (2010) investigated the behaviour of two traditional king-post trusses on a full-scale load-carrying test under symmetric and asymmetric loading, to identify suitable reinforcement methods. Barbari et al. (2014) tested a full-size prototype of a traditional timber truss, to verify the mechanical behaviour of an original joint connection system between the top-chord and the tie beam. More recently, two collar trusses were extensively assessed by visual inspection/grading and by NDTs before full-scale load-carrying tests by Branco et al. (2017). The trusses were first tested until failure in their present condition and then tested again after applying two different types of repairs. The interventions consisted on the strengthening of the support regions and local repairs at the failure areas of the rafters using either screwed timber elements or metal plates.

In-situ working conditions are a barrier and the setup implementation (measurement system and load application) is often difficult.

This work presents the field test results of a timber queen-post truss subjected to symmetric and non-symmetric loading. In this testing campaign the influence of the number of loading points was also studied. The truss has been characterized with regard to its geometry, material properties, material decay by using non-destructive tests methods. A numerical analysis has been developed to reproduce the test results.

2 TRUSS ASSESSMENT

The evaluated queen-post timber truss belongs to the roof structure of an old warehouse of Adico industry, located in Avanca (55 km South from Oporto). The exact date of the construction of the warehouse is not known but the Adico industry exists since 1920 and some plans of the village from 1942 already include the warehouse.

Trusses are the main elements of the roof structure, covered with ceramic tiles, 27º slopes and rafters spaced 50 cm over the purlins and the ridge. The free span of the trusses is 11.8 m and the average distance between them is 3.5 m.

The geometry of this particular truss is out of the ordinary: its configuration is typical of a king-post truss, but the queen-posts were added by connecting the joint strut/rafter to the tie-beam. This is not the traditional queen-post truss geometry, in which the king-post is substituted by a straining beam connecting horizontally (in the superior part) the two queen-posts, those located below the higher purlin, and the struts connecting the bottom part of the queen-posts to the lower purlins. Clearly, it is an example of a timber truss with an incorrect configuration for the span of the roof. The correct queen-post truss geometry should have been used or two extra posts (princess-posts) should have been placed below the lower purlin. Point loads out of the joints, causing bending moments in the rafters, are the most common error detected in the preliminary survey performed in previous steps of the research program (Branco et al. 2006).

The truss is made out of maritime pine (*Pinus pinaster Aiton*). The timber members of the truss are slender which is a characteristic of traditional Portuguese roofs structures,

with cross-sections varying from 80x145 mm^2 for the struts to 80x220 mm^2 for the tie-beam. The tie-beam is suspended to the posts by iron straps nailed into the posts. Between the tie-beam and the king-post there is a gap of 5 cm while queen-posts are in contact with the tie-beam. Connections between the other timber members are made by single step joints, in some cases nailed, and the queen-posts/rafters connections have a nailed heel strap connecting the post to the rafter (25 mm wide and 5 mm tick), Figure 1.

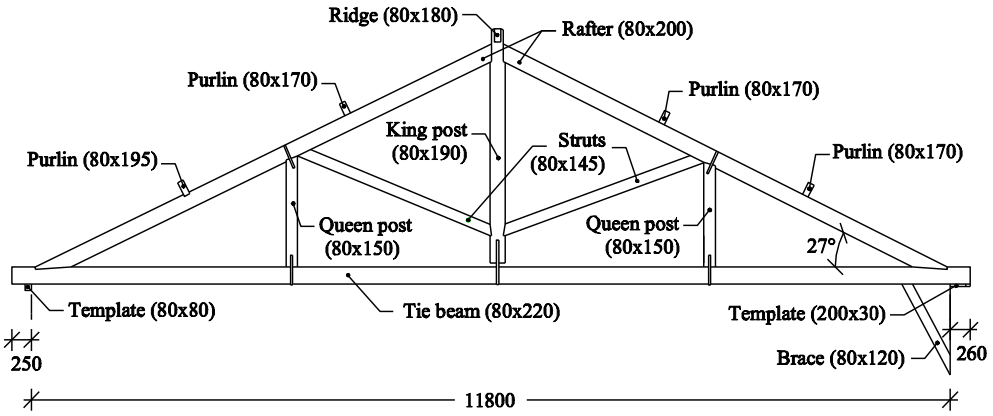

Figure 1. Truss geometry (dimensions in mm).

Despite the apparent good condition of the timber members of the truss, visual inspection revealed damage caused by insect attacks to the tie-beam, queen-posts and struts. In these timber members, emergence holes over the surface of sapwood are visible. However, no signs of active infestation were detected (Figure 2).


Figure 2. Emergence holes over the surface of sapwood.

Pilodyn® and Resistograph® non-destructive tests were performed to evaluate the extension of the decay in the timber truss (Figure 3). The Pilodyn 6J was used with the aim to assess the surface hardness through the depth penetration of the pin steel (2.5 mm) measured in each performed test. Resistograph permits to plot profiles (drill resistance versus penetration depth) that can be used to determine the location and extent of voids, allowing for the calculation of the residual cross section, Figure 4, (since decayed wood presents lower penetration resistance), and variation in material density.

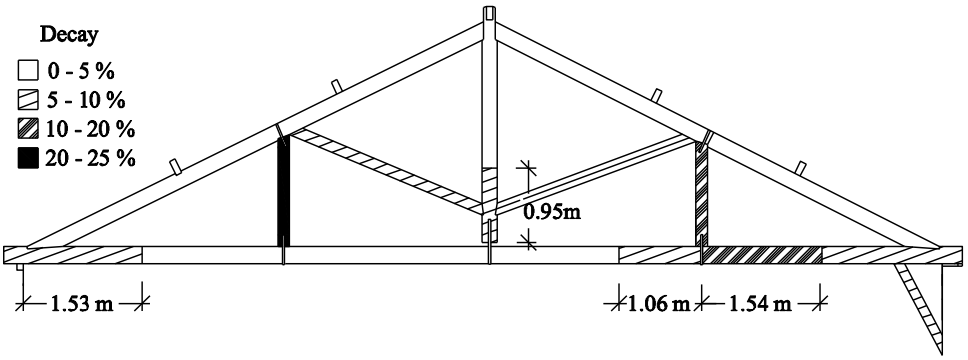

Figure 3. Map of the decay extension in the truss.

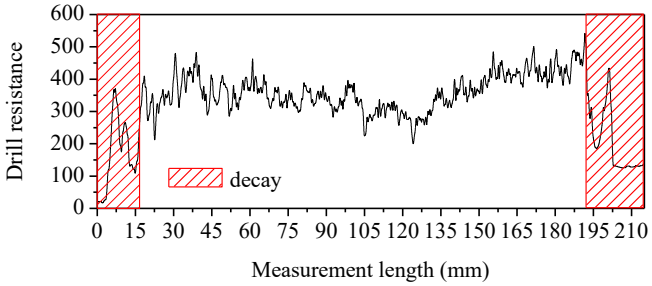

Figure 4. Example calculation of cross-section reduction based on a Resistograph test profile.

3 TEST SETUP, INSTRUMENTATION AND PROCEDURE

The main goal of the tests was to evaluate the overall behavior of the selected timber truss under symmetric and non-symmetric loading. Moreover, the influence of the location of the applied point loads, with and without eccentricity relatively to the joints, was assessed. This is the consequence of the geometry of the roof, which exhibits two purlins located with an eccentricity relatively to the intermediate joint of the rafter. Therefore, firstly, in the first test, joints loads were applied in the joints (locations F1, F2 and F3 - see Table 1) and, secondly, in the second test, loads were applied over the purlins and the ridge (locations F1, F4, F5, F6 and F7). Loading and unloading were recorded and an attempt to measure the deformation under constant loading conditions of the structure under symmetric loading was made. The behaviour of the truss under non-symmetric loading was evaluated, in the first scheme (3 point loads), only by one test and in the second (5 point loads) with two tests (one in each pitch side). Table 1 resumes the on-site load-carrying tests performed.

Table 1. Summary of the tests performed.

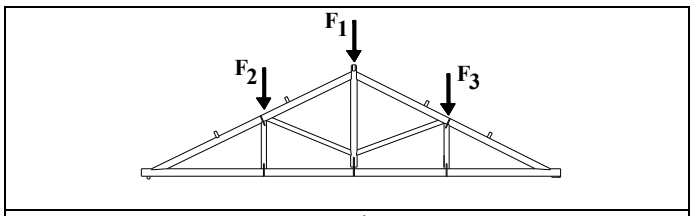	Procedure

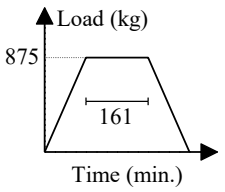

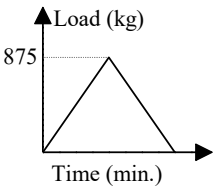

Test	Point loads	Test	Point loads
3FC	F_1, F_2 and F_3	3FN	F_3

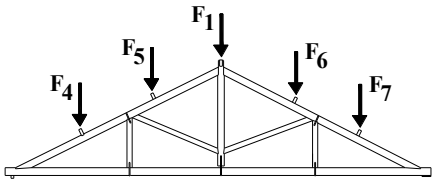

Procedure

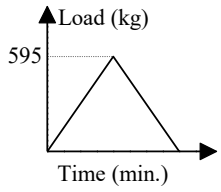

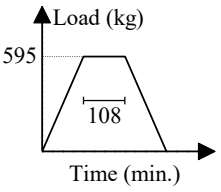

Test	Point loads	Test	Point loads
5FS	F_1, F_4, F_5, F_6 and F_7	5FC	F_1, F_4, F_5, F_6 and F_7
5FN1	F_6 and F_7		
5FN2	F_4 and F_5		

Wood pallets suspended to the truss by four steel cables (ϕ 6 mm) supported the load (materailized by 35 kg cement bags). Each loading and unloading path was divided into steps of 175 kg (5 bags). A total load of 2625 kg (3 x 875 kg) and 2975 kg (5 x 595 kg) was used in the first (three point loads) and second (five point loads) schemes, respectively. The difference in maximum loading applied with the two schemes, i.e. 350 kg, is due to the difficulty of increasing the number of bags placed over the pallets in the first case. To record the displacements of the truss during the tests, eight LVDTs (Linear Variable Differential Transformer) and six dial gauges (DG) were used. LVDTs were adopted to measure the global displacement (LVDTs 1 to 3), the behavior of the king-post/tie-beam connection (LVDT-5), the displacement below the purlins (LVDTs 4 to 8) and were also used to calculate the rotational behavior of the joints rafter/tie-beam and rafter/strut. The relative displacements at the LVDTs during the tests were acquired by a Data Acquisition System, with 8 channels, using a Lab-VIEW program (version 8.2). Dial gauges measured the opening of the queen-post/tie-beam con-nections (DG-3 and 4), the horizontal displacement of the rafter in the rafter/tie-beam connections (DG-5 and 6) and two additional points to calculate the rotation of rafter/tie-beam connections (DG-1 and 2). Figure 5 shows the instrumentation layout used in the tests performed.

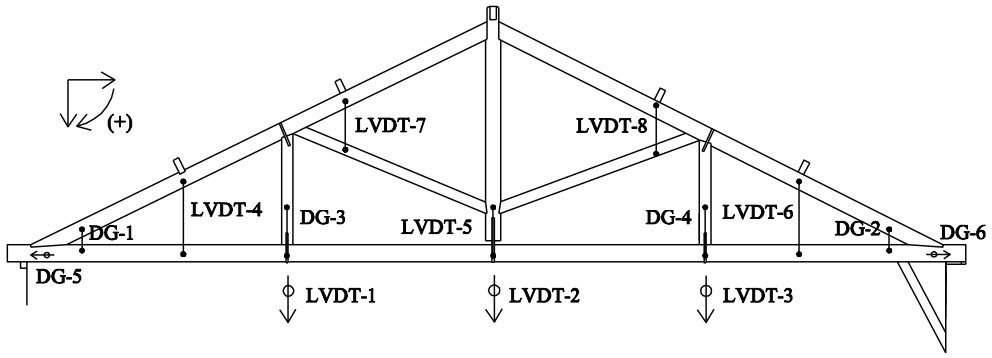

Figure 5. Instrumentation of the tests. Eight LVDTs and six DGs.

In every loading and unloading step the displacement values of the LVDTs were recorded. However, in the case of the DGs, only some steps were acquired, as a result of the reduced variation observed.

4 ANALYSIS OF THE TEST RESULTS

The behavior of the traditional timber trusses even under symmetric loading tends to be non-symmetric. The response of traditional timber trusses highly depends on: the variability of the timber member cross-sections, material properties, connections, supports and loading conditions. When using a natural and anisotropic material like wood, it is impossible for carpenters during construction, sometimes in extremely difficult working conditions, to avoid that variability. Moreover, in the case of old constructions, this heterogeneity and differences are more emphasized due to decay processes and lack of maintenance.

The field test results confirm that the truss under investigation presents a non-symmetric behavior even when subjected to symmetric loading conditions (Figure 6).

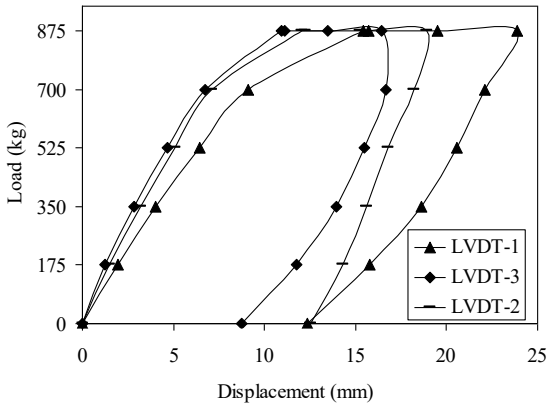

Figure 6. Displacement recorded by LVDTs 1, 2 and 3 during 3FC test.

The difference observed between the displacement-load curves of LVDT's 1, 2 and 3 can represent the influence of the decay observed in the left queen-post. The constant load rate applied during 161 minutes (see Table 1) results in a deformation increment of the truss (deformation under constant loading conditions). The truss presents important permanent deformations (average value of 57%) after the complete unloading. The

king-post/tie-beam connection works effectively, i.e. the tie-beam is suspended to the king-post (Figure 7).

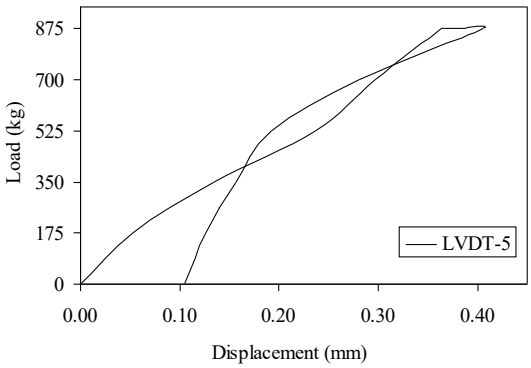

Figure 7. Behavior of the king-post/tie-beam connection during 3FC test.

The heel strap is able to suspend the tie-beam, therefore reducing the deformation of this element (see LVDT-2 in Figure 6), and also presents deformation under constant loading conditions. However, it is lesser than the one presented by the wood members. The connections between the queen-posts and the tie-beams, where a heel strap suspended the tie-beam, show different behaviors (Figure 8). Only the left connections, measured by DG-3, in the second series of tests (5F, 5 point loads – 5FS), behave as expected – the tie-beam is suspended to the queen post. In the first series of tests, both tie beam-queen post connections present residual deformations as a clear indication that, prior to testing, those connections had been dismantled. The first series of tests were sufficient for the left connections to recover, while the gap between both connected elements existing in the right connection was not recovered (recorded by DG-4).

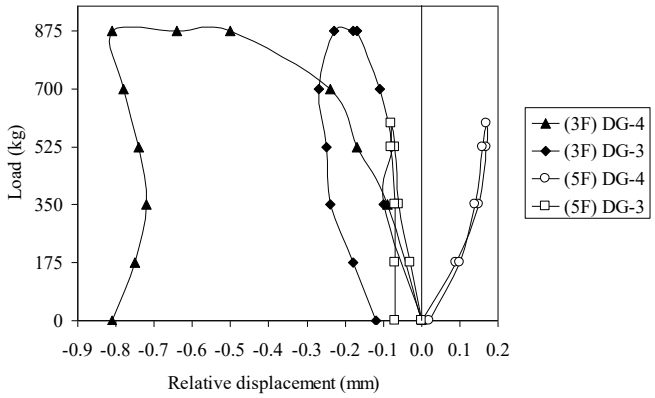

Figure 8. Behaviour of tie beam-queen post connections during 3FC and 5FS tests (Negative values are recorded when the two connected elements are approaching).

During the 3FC test, significant damage was detected on the left rafter/tie-beam connection, over the DG-5 (Figure 9a). Damage started at a point load level of 2100 kg. When 2550 kg of load was reached, DG-5 measurements were unstable (increasing with a constant rate) during 30 minutes. At the end of the loading period, a maximum relative horizontal displacement between the rafter and the tie-beam (measured by DG-5) was reached and without recovering during and after the unloading path (see Figure 9b).

a) Damage at 2550 kg of loading

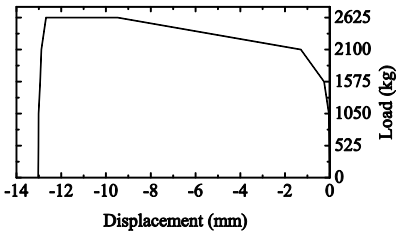

b) Load-displacement curve of DG-5

Figure 9. Behavior of the left rafter/tie-beam connection during 3FC test.

Under non-symmetric loading, as the one imposed during the test 3FN, distortion of the truss was observed, in particular, in the tie-beam, as shown in Figure 10. Non-symmetric behavior is evidenced by the signals acquired by LVDT-1 and 3 with lower values in the first LVDT as consequence of a higher stiffness (compression of the left queen-post).

Dividing the total amount of load applied by more point loads in the second tests series, from 3 to 5, the same general conclusions about the asymmetric behaviour of the truss, even when subjected to symmetric loading, can be drawn. The main difference between the tests under 3 and 5 point loads is, in the second case, the introduction of significant bending deformations in the rafters.

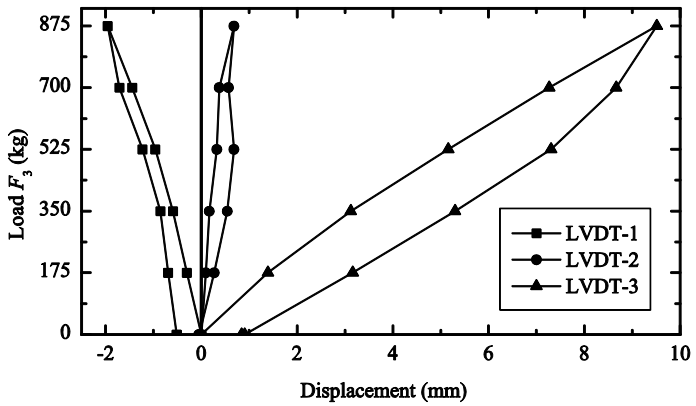

Figure 10. Displacement recorded by LVDTs 1, 2 and 3 during 3FN test.

In the second series of tests, larger values of rotation in the connections are obtained (Figure 11) while the global displacements are lower (Figure 12), when compared with the 3 point loads case. In the first case the system is more rigid.

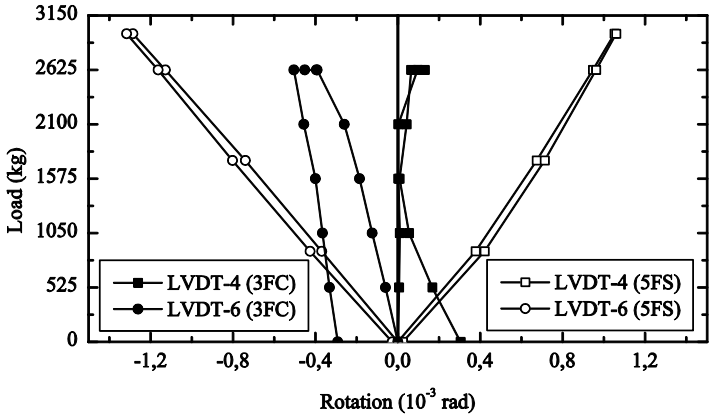

Figure 11. Comparison between rotations calculated based on values recorded by LVDTs 4 and 6 during 3FC and 5FS tests.

Applying the loads with eccentricity relatively to joints, the main deformations are found in the rafters, caused by bending, and greater rotations of the rafter/struts and rafter/tie-beam are obtained. When the point loads are applied directly at the joints, the main deformations are observed in the queen-posts (compression), pushing the tie-beam down. As a consequence, LVDTs 1, 2 and 3 show higher values of displacement (Figure 12). In addition, the deformation under constant loading conditions observed in the case of the three point loads (3F C) is significantly greater but, in this case, the influence of the damages observed in the rafter/tie-beam connection must be taken into account.

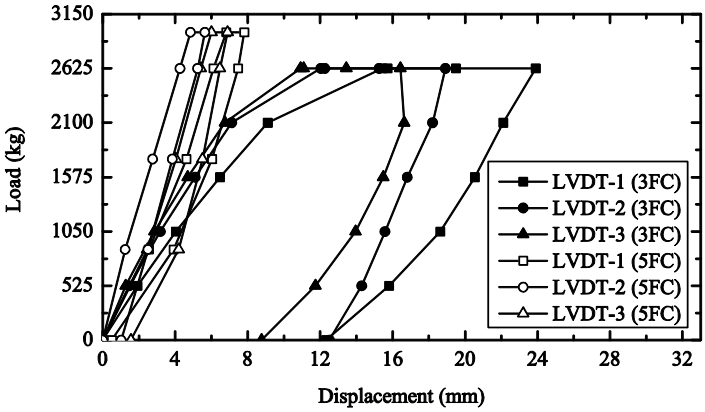

Figure 12. Comparison between the displacements recorded by LVDTs 1, 2 and 3 during 3FC and 5FC tests.

5 NUMERICAL ANALYSIS

The structural analysis program SAP 2000 was used to model the tests carried out. Linear beams elements, assuming the material properties suggested by LNEC (1997) for the Maritime pine wood, connected through semi-rigid joints modelled using nonlinear link elements (Nlinks), were used. The Nlinks elements, used in all connections between timber structural elements of the truss, placed at the extemities of the connected elements with a negligible length, are characterized by axial stiffness (see eqn (5)) and rotational stiffness defined by means of a Moment-Rotation (M-Φ) law proposed in Branco (2008). The conclusions from the preliminary inspection and the evaluation phase carried out

were introduced in the model, in particular, cross-sections were reduced according to the map of decay (see Figure 4).

5.1. Material model

Timber is assumed as an orthotropic material in the system so-called anatomic cylindrical coordinates corresponding to the longitudinal, *L*, radial, *R*, and transversal, T, directions of the tree trunk. Cylindrical coordinates may be approximated as orthogonal, for the material extracted from the outer region of the trunk. The elastic modulus, for an asymmetric model, are E_0 in the direction along the fibers, and E_{90} orthogonal to it, plus a shear modulus, G, and a Poisson's ratio, υ. For the material properties, the values presented in LNEC (1997) were adopted.

5.2 Geometric and mechanical models

The geometry and loading of the truss permits the assumption of a state of plane stress for the model. The truss is analyzed as a frame structure, adopting for all members elastic behavior while a semi-rigid behavior has been assumed for the connections. The semi-rigid behavior of the connections is introduced in the model with the Nonlinear link elements (Nlink).

5.3 Loads

To simulate the testing conditions, two types of loads were applied to the structure. Uniformly distributed loads representing the self-weight of the truss members, automatically computed, and joint loads as a result of the self-weight of the roof structure, transmitted to the truss by the purlins, and the ones applied during the different tests performed.

5.4 Semi-rigid modeling of connections

Traditional timber joints, even without any strengthening device, usually have a significant moment capacity. Indeed, common constraint models, like hinges or full restraint connections, cannot satisfactorily describe the real behavior of these joints. The joint behavior may be classified as semi-rigid and, being based on friction, is influenced by the time-varying level of compression between the joined members (Parisi & Piazza 2000). In order to properly describe this behavior, the elastic stiffness of each *Nlink* must be defined, according to the different geometric and mechanical features of the elements at each joint.

Candelpergher & Piazza (2001) have proposed expressions to define the rotation stiffness of traditional timber connections. However, these rules should be verified in the case of the Portuguese traditional timber connections. Because this calibration process is not yet finished, only the symmetric tests were numerically analyzed. In the case of the symmetric tests performed, the rotation stiffness of the connections has a trivial influence in the overall behavior of the tested truss. However, the axial stiffness of the connections is crucial in the truss response (deformation and stress distribution).

The axial stiffness (k_{ax}) depends of the timber mechanical properties, the geometric proportions of the connected elements and the connection angle (skew angle):

$$k_{ax} = \frac{E_{\alpha} S}{l} \tag{1}$$

where, applying the Hankinson Equation (2):

$$E_{\alpha} = \frac{E_0}{\cos^2 \alpha + \frac{E_0}{E_{90}} \sin^2 \alpha} \tag{2}$$

E_{α} represents the wood elastic modulus in the direction forming an angle α with the fiber.

$$l = \frac{h}{2 \sin \alpha} \tag{3}$$

l represents the nominal notch length, where compression deformation occurred.

$$S = \frac{A_{rafter}}{\sin \alpha} \tag{4}$$

S represents the nominal notch area, where stress was assumed to be transmitted.

The axial stiffness of the tie-beam/posts connections ($k_{ax,hs}$) has been formulated taking into account the axial stiffness of the heel strap:

$$k_{ax,hs} = \frac{E_{steel} A_{heel\ strap}}{l_{heel\ strap}} \tag{5}$$

where E_{steel} is the modulus of elasticity of steel, $A_{heel\ strap}$ and $l_{heel\ strap}$ is the cross-section and the length of the heel strap, respectively.

6 COMPARISON BETWEEN NUMERICAL AND EXPERIMENTAL RESULTS

Numerical modeling and experimental results have been compared. At first, pre-test analyses were developed, designated as Step 0, in which the numerical model has been implemented without considering the behavior of the truss observed in the performed tests. Then, the model was verified and calibrated based on the tests results (Step 1). Symmetric tests were used essentially to calibrate the axial stiffness of the connections while rotational stiffness have been adjusted with asymmetric tests results. In the following the main conclusions of the model ability to reproduce the experimentl results is discussed and the conclusions are presented.

6.1. Symmetric loading tests

Using the calculated axial stiffness for the connections, in Step 0, the computed values for the global displacements (at locations of LVDT 1 to 3) represents only 33% of the test results obtained for the first test (3FC). This difference is justified by the evidenced initial gap in all connections, in particular the ones between the posts and the tie beam.

Previously to the tests, significant gaps were observed between the metal devices and the joint. Moreover, the deterioration and strength reduction of the steel elements are not considered in the calculated stiffness values. The gaps between the metal devices and the joints are confirmed by the tests results (see Figures 7 and 8). It is also important to point out that the plastic deformation measured in the global displacement after the 3FC test represents 52%, 66% and 53% of the maximum displacement, respectively for LVDT 1, 2 and 3. In the case of the relative displacements measured in the tie beam-posts connections, the residual values represents 57%, 100% and 52% of the maximum displacement recorded at LVDT-5, DG-3 and DG-4, respectively. Therefore, the stiffness values calibrated for the first tests performed, 3FC, should be only considered as informative, because they report the influence of the original gaps existing between the metal devices and the joints. It is important to note that during the first test, 3FC, a significant damage of the left rafter-tie beam connections was detected (Figure 9) which influences directly the global displacements values. However, the calibrated model was able to reproduce the non-symmetric response of the truss even under symmetric loading conditions applied during the 3FC test (Figure 13).

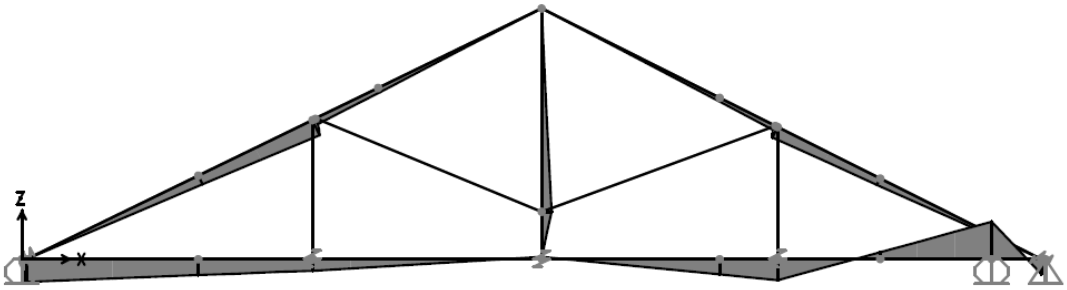

Figure 13. Bending moment on the truss elements in the 3FC test.

Table 2 gives a comparison between the experimental and numerical results (SAP 2000) for both symmetric loading tests performed, namely for the displacements in the joints of the truss. The values reported in Table 2 are the maximum displacement for the symmetric loading tests performed.

Table 2. Comparison between numerical results (Num.) and test results (Exp.). Error (Er.) expressed in (%).

Test 3FC								
Global displacements (mm)								
LVDT-1			LVDT-2			LVDT-3		
Exp.	Num.	Er.	Exp.	Num.	Err.	Exp.	Num.	Err.
15.40	15.25	0.90	12.00	13.71	14.30	10.90	9.64	11.60
Relative displacements – tie-beam/posts connections (mm)								
DG-3			LVDT-5			DG-4		
Exp.	Num.	Er.	Exp.	Num.	Err.	Exp.	Num.	Err.
-0.64	-0.69	2.80	0.36	0.35	2.80	-0.18	-0.17	7.40
Relative displacements – rafters/tie-beam connections (mm)								

DG-5			DG-6		
Exp.	Num.	Er.	Exp.	Num.	Err.
-0.25	-0.26	4.60	0.18	0.19	6.70

Test 5FS								
Global displacements (mm)								
LVDT-1			LVDT-2			LVDT-3		
Exp.	Num.	Er.	Exp.	Num.	Err.	Exp.	Num.	Err.
7.53	7.98	6.00	4.48	4.94	10.3	5.30	5.40	2.00
Relative displacements – tie-beam/posts connections (mm)								
DG-3			LVDT-5			DG-4		
Exp.	Num.	Er.	Exp.	Num.	Err.	Exp.	Num.	Err.
-0.17	-0.18	7.60	0.14	0.14	2.90	0.07	0.07	4.30
Relative displacements – rafters/tie-beam connections (mm)								
DG-5			DG-6					
Exp.	Num.	Er.	Exp.	Num.	Err.			
-0.28	-0.30	7.10	0.11	0.10	7.00			

Table 2 shows a good match between the values derived from the numeric model and the values observed in the tests results. Apart from the the values recoreded in the LVDTs 2 and 3 values, all errors reported by the numeric model are under 10%. Experimental results for the global vertical displacement of the truss under the king post are clearly overestimated by the model. This inconsistency can be explained by the faulty connections between the king post and the tie beam. The heel strap must introduce a "frictional stiffness" which reduces the mid-span deformations of the tie beam when the truss is loaded. Ideally, in tie beam-post connections it shall be used a heel strap, nailed only in the post, suspending the tie beam with a connection without bending stiffness.

The calibration process of the numeric model shows that during the experimental campaign a stiffness increase of the connections occurred (Table 3). This conclusion, confirmed by the test results (see Figure 12), is due essentially to the fact that the connections were originally dismantled (significant gaps originally existed between the metal devices and the joints).

Table 3. Axial stiffness values (kN/m) used in the numerical model.

Test	DG-5	DG-6	DG-3	DG-4	LVDT-5
3FC	2900	74002	2000	2400	3200
5FS	721155	374000	1000	31500	10200

By using the numerical models calibrated on the symmetric test results, to simulate the non-symmetric loading conditions, a significant discrepancy was obtained between the numeric and experimental results. In particular, the global displacements at points LVDT-1, 2 and 3, and the connections between the tie beam and the posts, recorded by DG-3, DG-4 and LVDT-5 are sensitive to the connections rotational stiffness.

6.2. Non-symmetric loading tests

After the calibration of the connection axial stiffness, based on the test results achieved through the symmetric loading tests, non-symmetric loading tests were used to assess the influence of the rotational connection's stiffness over the overall behaviour of the truss, in particular, under non-symmetric loading conditions. In this process, the chronology of the tests was considered, assuming the axial stiffness values as the ones calibrated with the model corresponding to the previous symmetric loading test. Therefore, in the model concerning the 3FN test, the axial stiffness assumed for the connections were derived from 3FC test and, the values assumed in the models of 5FN1 and 5FN2 tests, were based on the axial stiffness values calibrated through the numeric model of 5FS test. However, during the calibration process of the numeric model for the 3FC test case, it was necessary to update the axial stiffness of some connections. That fact allows to conclude that, after 3FC test, the response of the connections were still unstable, still depending on the gaps existing between the connected surfaces, like the calibration process of the axial stiffness of the connections have shown (see Table 3). During the test history performed, the gaps of the connections were reduced and the axial stiffness of the connections increased. Table 4 shows the axial stiffness values updated during the calibration process of the model corresponding to 3FN test.

Table 4. Axial stiffness values (kN/m) used in the numerical model to simulate the test 3FN

Test	DG-5	DG-6	DG-3	DG-4	LVDT-5
3FN	292108	17000	4000	7000	16000

In the numeric modelling of the tests carried out, the rotational stiffness properties assumed were directly derived from the research steps presented in previous works, in particular, Branco (2008). Bilinear M-Φ laws were assumed for the Nlinks elements responsible to model the semi-rigid behaviour of the connections. The model results were compared with the test results and a sensitivity study of the connections rotational stiffness value was performed. Therefore, in addition to the suggested values by this research, the two extremes rotational stiffness models, rigid joints and perfect hinges, were evaluated. As expected, the connections rotational stiffness can be important under non-symmetric loading conditions and negligible for symmetric loading conditions. The numeric results (Figure 14) shows that the influence of the rotational stiffness assumed for the connections under symmetric loading conditions (3FC and 5FS tests) is negligible. The rotational stiffness assumed for the connections can change the deformation of the truss but, those variations are not important. The same is not true for tests under non-symmetric loading conditions. Figure 15 shows that the rotational stiffness assumed for the connections as direct consequences in the truss overall behaviour under non-symmetric loading tests.

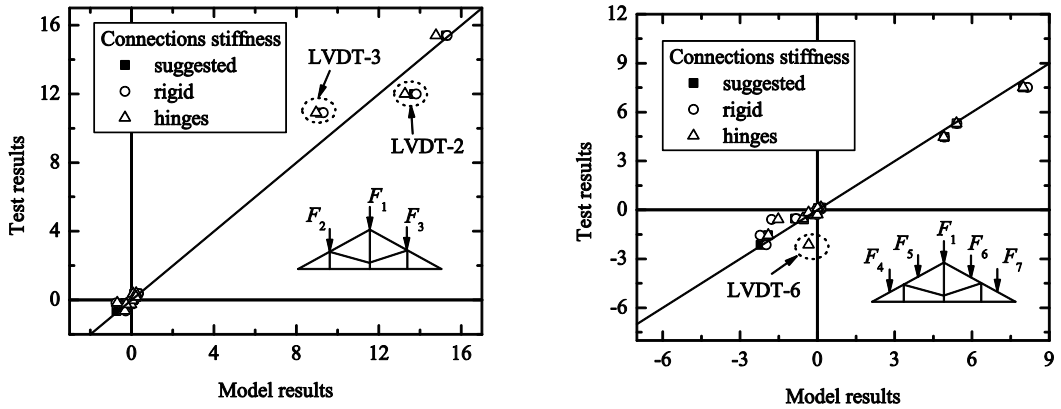

(a) 3FC (b) 5FS

Figure 14. Influence of the rotational stiffness of connections in the numerical results in comparison with test results under symmetric loading.

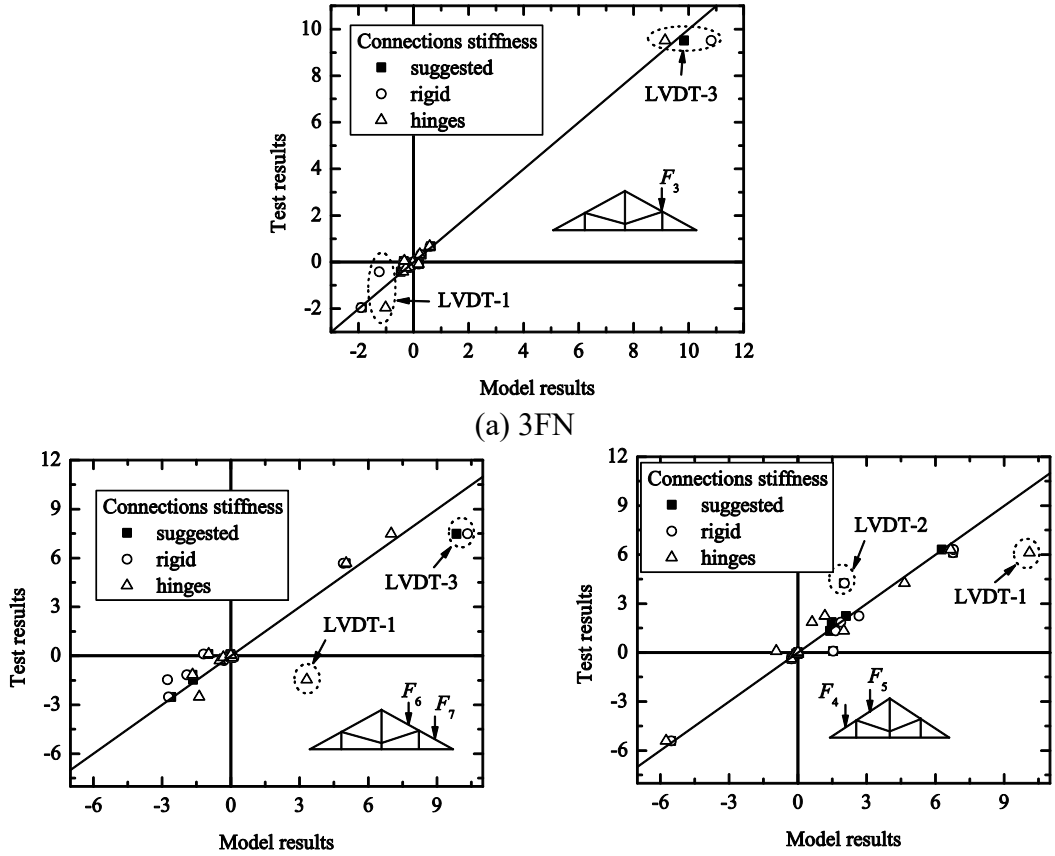

(a) 3FN

(b) 5FN1 (c) 5FN2

Figure 15. Influence of the rotational stiffness of connections in the numerical results in comparison with test results under non-symmetric loading.

The importance of the connections rotational stiffness in the truss overall behaviour raises with the truss distortion introduced during the tests. In the case of 5FN1 and 5FN2 tests, in which the truss distortion caused by the tests increases, the response of the truss becomes more dependent from the rotational stiffness properties adopted for the connections. In particular, the global displacement of the truss, measured by LVDT's 1,

2 and 3, are sensitive to the connection rotational stiffness. The variations reported by numeric modelling are not only in the displacement value measured but, as in the case of LVDT-1 during the 5FN1 tests considering rigid connections, in the signal. In this particular case, while the test result for the LVDT-1 is -1.452 mm (the minus sign corresponds to a lift of the point) the model with rigid joints presented a +3.317 mm displacement for the same point. This modification in the deformation of the truss had natural consequences over the stresses distribution, despite no significant variations in the stress maximum values were observed.

7 CONCLUSIONS

The results obtained from this work highlight the importance of the on-site experimentation in order to: 1) assess the global behaviour of traditional timber trusses by taking into account the real behaviour of the structural elements and their connections; 2) identify the critical areas; 3) plan the retrofit interventions and quantify their effects.

The experimentation developed gave an insight into the real truss behaviour, hardly reachable otherwise. The effects of the incorrect truss configuration for the roof span, the faulty connection geometry and the existing gaps in the joints over the overall behavior of the tested truss were assessed.

The numeric model implemented using the finite element code (SAP 2000) has proved to be effective and accurate in modelling the timber truss behaviour, considering semi-rigid behaviour for these traditional connections.

The comparison between the test results and the outcomes from the numerical models shows that the rotational stiffness assumed for the connections has particular importance for the truss behaviour in terms of deformations under non-symmetric loading conditions, and the influence of this condition becomes larger as the distortion introduced into the truss increases.

REFERENCES

Barbari M., Cavalli A., Fiorineschi L., Monti M., Togni M. (2014). Innovative connection in wooden trusses. Construction and Building Materials, 66, pp. 654-663. doi: 10.1016/j.conbuildmat.2014.06.022.

Branco J.M., Cruz P.J.S., Piazza M. & Varum H. 2006. Portuguese Traditional Timber Roof Structures, In WCTE 2006 - World Conference on Timber Engineering, 6-10 August, Portland, Oregon, USA.

Branco J.M. (2008), Influence of the joints stiffness in the monotonic and cyclic behavior of traditional timber trusses. Assessment of the efficacy of different strengthening techniques. Cotutelle PhD on Structural Engineering by University of Minho (Portugal) and University of Trento (Italy).

Branco J.M., Cruz P.J.S. & Piazza M. 2008. Diagnosis and analysis of two king-post trusses, In SAHC 2008: Structural Analysis of Historical Constructions, Bath, UK, 02-04 July.

Branco J.M., Varum H., Ramisote V., Costa A. (2016), Load-carrying capacity test of a long-span timber truss. Structures and Buildings. 2016, 169(5), pp. 373–387.

Branco J.M., Sousa H.M., Tsakanika, E. (2017), Non-destructive assessment, full-scale load-carrying tests and local interventions on two historic timber collar roof trusses. Engineering Structures. 2017, 140, 209–224.

Candelpergher L. & Piazza M. 2001. Mechanics of traditional connections with metal devices in timber roof structures. In Proceedings of the Seventh International Conference STREMAH 2001, Bologna, Italy.

Del Senno M. & Piazza M. 2003. Behaviour and rehabilitation of queen post timber trusses. A case study. In STREMAH 2003: Structural Studies, Repairs and Maintenance of Heritage Architecture VIII, May, Halki-diki, Greece.

LNEC. 1997. Timber for structures – Maritime pine for structures. LNEC (eds), Ficha M2. ISSN 0873-6472, Lisbon, 12 p. (only available in Portuguese).

Parisi M.A. & Piazza M. 2000. Mechanics of plain and retrofitted traditional timber connections. Journal of Structur-al Engineering, ASCE; 126(12): 1395–403.

Parisi M.A., Piazza M. (2002). Seismic behavior and retrofitting of joints in traditional timber roof structures. Soil Dynamics and Earthquake Engineering, 22, pp. 1183-1191. doi: 10.1016/S0267-7261(02)00146-X.

Piazza M., Brentari G. & Riggio M.P. 2004. Strengthening and control methods for old timber trusses: the queen-post truss of the Trento theatre. In SAHC 2004: Structural Analysis of Historical Constructions, Padova, IT, II: 957-965.

SAP 2000. Static and Dynamic Finite Element Analysis of Structures. Structural Analysis Program. Computers and Structures. Inc., Advanced 9.03. California. USA.